

Performance of the Optical Parametric Generation in Nonlinear KTP Crystal at Nd:YAG Laser Pumping

V.N. Belyi, N.S. Kazak, V.A. Orlovich and B.B. Sevruk

*B.I. Stepanov Institute of Physics, NAS of Belarus, 70
F. Skaryna ave., 220072, Minsk, Belarus*

(Received 11 November 1999)

The tuning curves, angular and spectral phase-matching widths are calculated for all possible kinds of OPG in the principal planes of biaxial KTP crystal with Nd:YAG laser pumping at 1.064μ wavelength. The plots presented enable the maximal nonmonochromaticity and radiation divergence to be found for any value of the signal wave and different interaction types. A particular emphasis has been placed on the OPG investigation under the noncritical phase-matching conditions of the type II along x and y crystallographic axes. The effective nonlinear coefficients as a function of phase-matching angles are calculated in the KTP principal planes.

Key words: nonlinear crystal, laser, phase-matching.

PACS numbers: 42.65.Ky; 42.70.Nq; 42.60.Jf; 42.25.Bs; 42.25.Ja; 42.25.Lc

1 Introduction

Considerable recent attention has been focused on the utilization of nonlinear potassium titanyl phosphate (KTP) crystal for optical parametric generation (OPG). The KTP crystal features suitable tuning parameters in infrared and visible wavelength ranges ($0.3 \div 4.5 \mu\text{m}$) and as reported in [1, 2] has found extensive applications as an eye-safe radiation source. It also exhibits a large value of optical nonlinearity (higher than BBO and LBO crystals), relatively high nonlinear coefficients, broad spectral, angular and temperature band-widths, high optical damage threshold [3, 4] and mechanical as well as chemical stability. As was reported in [5, 6, 7, 8] the OPG-based radiation conversion was obtained in the laser-pumped KTP crystal at wavelengths 532 nm, 527 nm and ($720 \div 850$) nm, respectively. A particular attention was focused on the OPG for Nd:YAG laser radiation ($1.064 \mu\text{m}$) conversion to the eye-safe range ($1.5 \div 1.8 \mu\text{m}$) [1, 2, 9, 10, 11, 12, 13, 4]. However, the tuning features for different types of interaction in KTP crys-

tal at Nd:YAG laser pumping have not been completely investigated. Information on spectral and angular phase-matching widths in all possible tuning ranges in an explicit form is practically unavailable. At the same time these data are extremely necessary for the creation of highly efficient tunable frequency converters, especially in the eye-safe signal wavelength range. Together with medical aspects of the problem, an interest to the eye-safe laser sources is stimulated by their applications in range finders, lidar systems for environmental monitoring, wind velocity gages, etc. In this paper we present the results of the investigation of parametric conversion in the principal planes of Nd:YAG laser pumped KTP crystal. The expressions for calculation of phase-matching characteristics for all possible kinds of interactions of the II type are given. The comprehensive analysis of tuning curves together with angular and spectral phase-matching widths are carried out. The effective nonlinear coefficients are calculated as well.

2 Tuning dependencies for different types of parametric conversion

The KTP crystal is a positive biaxial crystal of the mm2 point symmetry group [3]. The refractive indices n_{\pm} of two isonormal linear-polarized waves propagating in an arbitrary direction determined by the unit vector $\mathbf{n}(n_1, n_2, n_3)$ of wave normal are given by [14]

$$n_{\pm}^{-2} = \varepsilon_2^{-1} + \frac{1}{2} \left(\varepsilon_1^{-1} - \varepsilon_2^{-1} \right) \times \left[[\mathbf{nc}_1][\mathbf{nc}_2] \pm \left([nc_1]^2 [nc_2]^2 \right)^{\frac{1}{2}} \right]. \quad (1)$$

In this equation the elements of the dielectric tensor ε_i expressed in the principal crystallographic axes satisfy the following condition $\varepsilon_1 < \varepsilon_2 < \varepsilon_3$. Therefore optical axes determined by the unit vectors c_1 and c_2 lie in the x-z principal plane under the following angle to z-axis:

$$V_z = \arctan \left[\frac{\varepsilon_2^{-1} - \varepsilon_1^{-1}}{\varepsilon_3^{-1} - \varepsilon_2^{-1}} \right]^{\frac{1}{2}}.$$

It is convenient to express the wave normal vector components through the polar θ angle and azimuth φ angles in the spherical coordinates: $n_1 = \sin \theta \cos \varphi$, $n_2 = \sin \theta \sin \varphi$, $n_3 = \cos \theta$.

Then we can rewrite the expression (1) in the following form

$$n_{\pm} = \sqrt{2} \left[a + A \pm \left(b^2 - 2bB + A^2 \right)^{\frac{1}{2}} \right]^{-\frac{1}{2}}, \quad (2)$$

where $a = N_x^{-2} + N_z^{-2}$, $A = \left(N_y^{-2} - N_z^{-2} \right) \cos^2 \theta - \left(N_x^{-2} - N_y^{-2} \right) \sin^2 \theta \cos^2 \varphi$, $b = N_x^{-2} - N_z^{-2}$, $B = \left(N_y^{-2} - N_z^{-2} \right) \cos^2 \theta + \left(N_x^{-2} - N_y^{-2} \right) \sin^2 \theta \cos^2 \varphi$, $N_x < N_y < N_z$ are the principal indices of refraction.

A general approach for calculating of the phase-matching angles in biaxial crystals is provided in [15]. The peculiarities of phase-matching calculations are described in [16, 17]. Expressions for phase-matching angles in the principal planes of biaxial crystal are similar to those for the uniaxial crystal [18, 19].

Let us consider the collinear parametric interaction of pump (ω_3, k_3) , signal (ω_1, k_1) and idler (ω_2, k_2) waves in the principal planes of biaxial KTP crystal. Hereafter it is assumed that $\omega_3 > \omega_1 > \omega_2$. The frequencies and wavenumbers are determined by the laws of energy and momentum conservation

$$\omega_3 = \omega_1 + \omega_2, \quad k_3 = k_1 + k_2. \quad (3)$$

Equations (3) could be rearranged with the help of refractive indices $n(\omega)$ [20]

$$\omega_1 [n(\omega_3) - n(\omega_1)] + \omega_2 [n(\omega_3) - n(\omega_2)] = 0. \quad (4)$$

As far as interacting waves propagate in the principal plane of biaxial crystal, their refractive indices are analogous to those of the ordinary wave (n_o) and extraordinary wave (n_e) in uniaxial crystal. Taking this similarity into consideration we would mark, in much the same way as in the paper [21], the wave polarized perpendicularly to the principal plane of the crystal by o index and by e index with parallel polarization. If inequality $n_e(\omega) < n_o(\omega)$ takes place in the principal planes of biaxial crystal, one could fit such conditions for the extraordinary pump wave to satisfy the equation (4). Usually two types of collinear phase-matching are considered. For the interaction of type I generated signal and idler waves have the same polarization and for the interaction of type II the polarizations of converted waves are opposite [20]. Thus $e_3 \rightarrow o_1 e_2$ and $e_3 \rightarrow e_1 o_2$ phase-matching is possible for the II type of interaction in a negative crystal. In the principal plane of biaxial crystal, where $n_o(\omega) < n_e(\omega)$ relationship is fulfilled, the condition (4) is valid for the ordinary pump wave as well. Therefore $e_3 \rightarrow o_1 e_2$ and $e_3 \rightarrow e_1 o_2$ phase-matching is possible for the II type of interaction in a positive crystal.

Let us investigate further tuning dependencies for collinear OPG, when the pump wave ($\lambda_3 = 1.064 \mu\text{m}$) propagates alternately in these principal planes. In this case we consider only II type of interaction, as for interaction of type I effective coefficients $d_{eff} \approx 0$ [16].

2.1 Phase-matching directions in the x-z plane of KTP crystal

Expressions for waves refractive indices in the x-z plane result from equation (2), if the azimuth angle is set to zero ($\varphi = 0$):

$$n_o = N_y, \\ n_e(\theta) = \left(N_z^{-2} \sin^2 \theta + N_x^{-2} \cos^2 \theta \right)^{-1/2} \quad (5)$$

Then the refractive index n_o for the ordinary wave polarized perpendicularly to the given plane (along the y-axis) is constant, while for the extraordinary wave polarized in the x-z plane, the refractive index $n_e(\theta)$ varies from N_x to N_z at variations of the θ angle from 0° to 90° . The KTP crystal is similar to a negative uniaxial crystal at $0 \leq \theta \leq V_z$, and at $V_z \leq \theta \leq 90^\circ$ - to a positive uniaxial crystal. Hereafter we consider tuning dependencies at $\theta \geq V_z$, as for the type II interaction in the x-z plane, $d_{eff} \sim \theta$ and the angle $V_z \approx 18^\circ$. The above described phase-matching conditions in this case are fulfilled for the type II interactions $e_3 \rightarrow o_1 e_2$ and $e_3 \rightarrow e_1 o_2$, when the pump wave is an ordinary wave with y-axis polarization.

For the $o_3 \rightarrow o_1 e_2$ type of interaction, when the o- pump wave is converted into o-signal and e-idler wave, the phase-matching conditions (3) may be written as

$$\frac{N_{y3}}{\lambda_3} = \frac{N_{y1}}{\lambda_1} + \frac{n_{e2}(\theta)}{\lambda_2}, \\ \lambda_2 = \lambda_1 \lambda_3 / (\lambda_1 - \lambda_3), \quad (6)$$

where $N_{xi} = N_x(\lambda_i)$, $N_{yi} = N_y(\lambda_i)$, $N_{zi} = N_z(\lambda_i)$ and $n_{ei} = n_e(\lambda_i)$ are the values of refraction indices at the wavelength $\lambda = \lambda_i$, $i = (1, 2, 3)$.

The tuning curves calculated with the help of (5, 6) are plotted in Figure 1 (solid and dashed curves 1). The calculations were carried out using Sellmeier equations

$$N_j^2(\lambda) = A_j + B_j \left(1 - C_j \lambda^{-2} \right)^{-1} - D_j \lambda^2, \quad (7)$$

where the equation coefficients are published in [3]. It can be seen from Figure 1 that by varying θ one can receive the relatively wide tuning ranges for the signal and idler waves for $o_3 \rightarrow o_1 e_2$ phase-matching at the x-z plane. The tuning curves intersect each

other at $\theta \cong 52^\circ$, i.e. a degenerate OPG with $\lambda_1 = \lambda_2 = 2.1 \mu\text{m}$ exists at this angle. In the vicinity of $\theta \cong 44^\circ$ a noncritical phase-matching is observed. It is convenient to make use of this feature for the parametric generation of short (picosecond) pulses in the vicinity of $1.5 \mu\text{m}$ and $3 \mu\text{m}$.

The phase-matching condition for the $e_3 \rightarrow o_1 e_2$ parametric conversion process in the x-z plane takes the form

$$\frac{N_{y3}}{\lambda_3} = \frac{n_{e1}(\theta)}{\lambda_1} + \frac{N_{y2}}{\lambda_2}. \quad (8)$$

Tuning dependencies calculated with the help of the equation (8) are practically identical to those plotted in Figure 1 (curves 1).

2.2 Tuning curves in the x-y plane of KTP crystal

The polar angle $\theta = \pi/2$ in the x-y plane and it follows from (2) that

$$n_o = N_z, \\ n_e(\varphi) = \left(N_x^{-2} \sin^2 \varphi + N_y^{-2} \cos^2 \varphi \right)^{-1/2}. \quad (9)$$

Thus, the refractive index n_o of the ordinary wave polarized along the z-axis is constant, while the refractive index $n_e(\varphi)$ of the extraordinary wave polarized in the x-y plane varies from N_y to N_x at variations of the φ angle from 0° to 90° . It follows, that KTP crystal in the x-y plane is similar to a negative uniaxial crystal. For this reason phase-matching conditions in the x-y plane are fulfilled for type II interactions, provided that the pump wave is an extraordinary wave: $e_3 \rightarrow e_1 o_2$ and $e_3 \rightarrow o_1 e_2$. For $e_3 \rightarrow e_1 o_2$ interaction, the equation (3) is written as

$$\frac{n_{e3}(\varphi)}{\lambda_3} = \frac{n_{e1}(\varphi)}{\lambda_1} + \frac{N_{z2}}{\lambda_2}. \quad (10)$$

The tuning curves resulted from (9, 10) and Sellmeier equations (8) are shown in Figure 1 (solid and dashed curves 2). It is evident, that variations of the azimuth angle ϕ in the x-y plane give the much less tuning range of the converted waves than that in the x-z plane (curves 1) That can be attributed to a relatively small double beam refraction

in the x-y plane (in comparison to the x-z plane) to compensate for dispersion in a wide spectral region. The calculations have shown that the tuning curves for another possible interaction in the x-y plane $e_3 \rightarrow o_1e_2$ are identical to those plotted in Figure 1(curves 2).

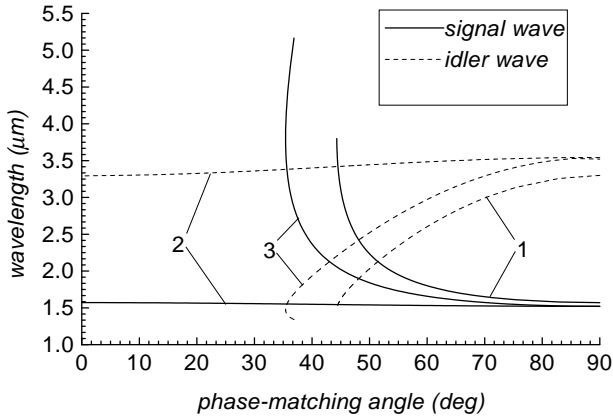


FIG. 1. Tuning curves for OPG in KTP crystal at Nd:YAG ($\lambda = 1.064 \mu\text{m}$) laser pumping: 1- $e_3 \rightarrow o_1e_2$ interaction in the x-z plane, 2- $e_3 \rightarrow e_1o_2$ interaction in the x-y plane, 3 - $e_3 \rightarrow e_1o_2$, y-z plane.

2.3 Tuning curves in the y-z plane of KTP crystal

Assuming in (2) that $\theta = \pi/2$, we get two type of waves propagating in the y-z plane of KTP crystal with refractive indices

$$n_o = N_x,$$

$$n_e(\theta) = \left(N_z^{-2} \sin^2 \theta + N_y^{-2} \cos^2 \theta \right)^{-1/2}. \quad (11)$$

Considering that the biaxial KTP crystal in the y-z plane is similar to a positive uniaxial crystal, the phase-matching for type II interaction will be achieved only for the ordinary pump wave polarized along the x-axis. We consider here the most interesting type of phase-matching $o_3 \rightarrow e_1o_2$, which has been utilized in the case of y-cut KTP crystal for Nd:YAG laser radiation conversion in the eye-safe range. Equations (3) for $o_3 \rightarrow e_1o_2$ phase-matching in the y-z plane of KTP crystal take the following

form

$$\frac{N_{x3}}{\lambda_3} = \frac{n_{e1}(\theta)}{\lambda_1} + \frac{N_{x2}}{\lambda_2}. \quad (12)$$

The tuning curves calculated with the help of (11, 12) and Sellmeier equations (8) are plotted in Figure 1 (solid and dashed curves 3). It could be seen that by varying θ angle one can get the relatively wide (as in the case of x-z plane) tuning range for signal e-wave and for idler o-wave. A degenerate parametric conversion with $\lambda_1 = \lambda_2 = 2.1 \mu\text{m}$ is achieved at $\theta \approx 43^\circ$. At $\theta \approx 36^\circ$ noncritical phase-matching for a wide wavelength region also exists, which is suitable for parametric picosecond pulse generation in the middle part of infrared region.

3 Phase- matching angular width and pump divergence requirements

A significant point in providing efficient parametric conversion is that the pump wave divergence should not exceed the phase-matching angle width [22]. A deviation from the phase-matching angle $\delta\theta = \theta - \theta_c$ for certain interaction type gives rise to a phase mismatch

$$\Delta k = \Delta k(0) + \frac{\partial(\Delta k)}{\partial\theta} \delta\theta + \frac{1}{2} \frac{\partial^2(\Delta k)}{\partial\theta^2} (\delta\theta)^2 + \dots \quad (13)$$

The phase mismatch value Δk for three-wave parametric conversion is determined via refractive indices n_i and wavelengths λ_i of the interacting waves [20]

$$\Delta k = 2\pi \left(\frac{n_3}{\lambda_3} - \frac{n_1}{\lambda_1} - \frac{n_2}{\lambda_2} \right). \quad (14)$$

Double radiation power reduction for signal wave takes place at phase mismatch $\Delta k = 0.886\pi/L$. Required phase-matching angle deviation according to (14) could be found from the following quadratic equation

$$(\delta\theta)^2 + 2p(\delta\theta) - q = 0, \quad (15)$$

with the coefficients $p = a_1 a_2$, $q = 0.886/a_2 L$, and $a_1 = (2\pi)^{-1} \partial(\Delta k)/\partial\theta$ and $a_2 = (2\pi)^{-1} \partial^2(\Delta k)/\partial\theta^2$.

3.1 Phase-matching angular width in the case of noncritical phase-matching

Noncritical phase-matching (NPM) for collinear OPG along x and y principal axes of KTP crystal exists in the case when the first derivative $\partial(\Delta k)/\partial\theta$ in (13) vanishes. The NPM is a very attracting phenomenon due to the absence of energy walk-off, extremal d_{eff} and considerable phase-matching angle width. The phase-matching angular width $\Delta\theta\sqrt{L} = 2\delta\theta\sqrt{L}$ for the NPM is determined according to (15) by the following expression [23]

$$\Delta\theta\sqrt{L} = 2\sqrt{1.772} \left(\frac{\partial^2(\Delta k)}{\partial\theta^2} \right)^{-1/2}. \quad (16)$$

On the basis of (16) one can get expressions for calculating of the angular phase-matching widths for x- and y-cut KTP crystal.

3.1a Acceptance pump divergence $\lambda_p = 1.064 \mu\text{m}$ for the x-cut KTP crystal

For the x-cut KTP crystal ($\varphi = 0^\circ$, $\theta = 90^\circ$) the pump ($\lambda_3 = 1.064 \mu\text{m}$) and signal ($\lambda_1 = 1.57 \mu\text{m}$) waves are polarized along y-axis and the idler ($\lambda_2 = 3.29 \mu\text{m}$) wave possesses z-axis polarization. The acceptance pump divergence for such OPG type in the xz-plane is determined by the angular width of the $o_3 \rightarrow o_1 e_2$ interaction, which, in accordance with (16), is equal to

$$\Delta\theta_x\sqrt{L} = 2\sqrt{0.886} \left[\frac{N_{z2}}{\lambda_2} \left(\frac{N_{z2}^2}{N_{x2}^2} - 1 \right) \right]^{-1/2}. \quad (17)$$

Quite similarly the acceptance pump divergence in the xy-plane is determined by the angular width of the $e_3 \rightarrow e_1 o_2$ interaction

$$\Delta\varphi_x\sqrt{L} = 2\sqrt{0.886} \times \left[\frac{N_{y1}}{\lambda_1} \left(\frac{N_{y1}^2}{N_{x1}^2} - 1 \right) - \frac{N_{y3}}{\lambda_3} \left(\frac{N_{y3}^2}{N_{x3}^2} - 1 \right) \right]^{-1/2}. \quad (18)$$

From (17) and (18) we obtain the following numerical values of angular acceptance pump divergence

for the x-cut KTP crystal of $L = 1 \text{ cm}$ length: $\Delta\theta_x = 84 \text{ mrad}$ in the xz-plane and $\Delta\varphi_x = 260 \text{ mrad}$ in the xy-plane.

3.1b Acceptance pump divergence ($\lambda_p = 1.064 \mu\text{m}$) for the y-cut KTP crystal

For the y-cut KTP crystal ($\varphi = 90^\circ$, $\theta = 90^\circ$) the pump ($\lambda_3 = 1.064 \mu\text{m}$) and idler ($\lambda_2 = 3.54 \mu\text{m}$) waves are polarized along x-axis and the signal ($\lambda_1 = 1.52 \mu\text{m}$) wave possesses z-axis polarization. The acceptance pump divergence for such OPG type in the yz-plane is determined by the angular width $\Delta\theta_y\sqrt{L}$ of the $o_3 \rightarrow e_1 o_2$ interaction

$$\Delta\theta_y\sqrt{L} = 2\sqrt{0.886} \left[\frac{N_{z1}}{\lambda_1} \left(\frac{N_{z1}^2}{N_{y1}^2} - 1 \right) \right]^{-1/2}. \quad (19)$$

Similarly to the previous case, the acceptance pump divergence in the xy-plane is determined by the angular width $\Delta\theta_\varphi\sqrt{L}$ of the $e_3 \rightarrow o_1 e_2$ interaction phase-matching, which, in accordance with (16) is equal to

$$\Delta\varphi_y\sqrt{L} = 2\sqrt{0.886} \times \left[\frac{N_{x3}}{\lambda_3} \left(1 - \frac{N_{x3}^2}{N_{y3}^2} \right) - \frac{N_{x2}}{\lambda_2} \left(1 - \frac{N_{x2}^2}{N_{y2}^2} \right) \right]^{-1/2}. \quad (20)$$

From (19) and (20) we find the following numerical estimations of acceptance angular divergence of Nd:YAG laser radiation for the y-cut KTP crystal of 1 cm length: $\Delta\theta_y = 56 \text{ mrad}$ in the xy-plane and $\Delta\varphi_y = 183 \text{ mrad}$ in the yz-plane.

3.2 Phase-matching angular width in the principal planes of KTP crystal

In the case when deviations from x- and y-axis take place, the major contribution to phase mismatch (13) comes from the term linear in $\delta\theta$ and the angular phase-matching width $\Delta\theta\sqrt{L} = 2\delta\theta\sqrt{L}$ is determined from (15)

$$\Delta\theta L = 0.886/|a_1|. \quad (21)$$

Let us write the explicit formula for the a_1 coefficient entering (21), as it is necessary for the calculating of the acceptance pump divergence of three

most efficient collinear OPG types in the principal planes of KTP crystal.

a) For the xz-plane ($\varphi = 0^\circ$) $o_3 \rightarrow o_1e_2$ parametric conversion:

$$a_1 = V_{e2}/\lambda_2,$$

$$V_{e2} = \left[\left(N_{x2}^{-2} - N_{z2}^{-2} \right) n_{e2}^3(\theta) \sin 2\theta \right] / 2 \quad (22)$$

b) For the xy-plane ($\theta = 90^\circ$) $e_3 \rightarrow e_1o_2$ parametric conversion:

$$a_1 = V_{e3}/\lambda_3 - V_{e1}/\lambda_1,$$

$$V_{e1} = \left[\left(N_{y1}^{-2} - N_{x1}^{-2} \right) n_{e1}^3(\varphi) \sin 2\varphi \right] / 2, \quad (23)$$

where V_{e3} could be found from (23) replacing index "1" by "3".

c) For the yz-plane ($\varphi = 90^\circ$) $o_3 \rightarrow e_1o_2$ parametric conversion:

$$a_1 = V_{e1}/\lambda_1,$$

$$V_{e1} = \left[\left(N_{y1}^{-2} - N_{z1}^{-2} \right) n_{e1}^3(\theta) \sin 2\theta \right] / 2. \quad (24)$$

The angular phase-matching width values $\Delta\theta L$ as a function of signal wavelength λ_1 calculated with the help of (22 - 24) for each OPG tuning range are plotted in Figure 2 (curves 1, 2, 3).

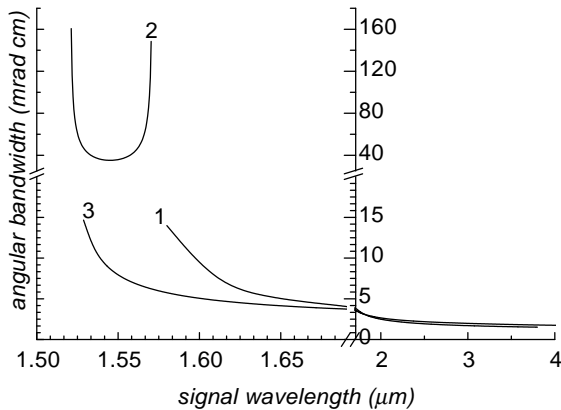


FIG. 2. Phase-matching angular width as a function of signal wavelength for OPG in KTP crystal at $\lambda_p = 1.064 \mu\text{m}$: 1- $o_3 \rightarrow o_1e_2$ interaction in the x-z plane, 2- $e_3 \rightarrow e_1o_2$, x-y plane, 3- $o_3 \rightarrow e_1o_2$, y-z plane.

As could be seen, $\Delta\theta L$ decreases with the deviation from x- and y-axis corresponding to NPM directions and varies insignificantly at signal wave variations from $2 \mu\text{m}$ to $4 \mu\text{m}$ for the xz-plane $o_3 \rightarrow o_1e_2$ and yz-plane $o_3 \rightarrow e_1o_2$ interactions (curves 1 and 3). For the xy-plane $e_3 \rightarrow e_1o_2$ interaction the range of small variations of angular phase-matching width $\Delta\varphi L$ goes from $1.525 \mu\text{m}$ to $1.565 \mu\text{m}$ (curve 2). These dependencies make it possible to determine the acceptance pump divergence for any signal wavelength value and various interaction types.

4 Phase matching spectral width

The acceptance pump wave nonmonochromaticity is determined by phase-matching spectral width. The pump wavelength variation $\delta\lambda_3$, at which the converted signal power decreases by a half, is given by the expression [22, 23]

$$\delta\lambda_3 = 0.886\pi \left(L \frac{d(\Delta k)}{d\lambda_3} \right)^{-1}. \quad (25)$$

It is believed that the acceptance pump wave nonmonochromaticity $\delta\lambda_3$ is twice as the $\delta\lambda_3$ value: $\delta\lambda_3 = 2\delta\lambda_3$. Taking this into consideration and using equations (25) and (14), one can get the following expression for the phase-matching spectral width

$$\Delta\lambda_3 L = 0.886\lambda_3^2 \left[\lambda_3 \frac{dn_3}{d\lambda_3} - n_3 - \frac{1}{2} \left(\lambda_1 \frac{dn_1}{d\lambda_1} - n_1 \right) - \frac{1}{2} \left(\lambda_2 \frac{dn_2}{d\lambda_2} - n_2 \right) \right]^{-1}. \quad (26)$$

Calculations of the phase-matching spectral width values $\delta\lambda_3 L$ as a function of signal wavelength λ_1 were provided on the basis of (26) for various OPG types in the principal planes of KTP crystal (at $\lambda_3 = 1.064 \mu\text{m}$). The results given in Figure 3 (curves 1, 2, 3) show, that KTP crystal possesses considerable phase-matching spectral width. For example, $\delta\lambda_3 L$ for $o_3 \rightarrow o_1e_2$ parametric conversion in the xz-plane (curve 1) and for $o_3 \rightarrow e_1o_2$ parametric conversion in the yz-plane (curve 3) ranges up to $\sim 10 \text{ nm}\cdot\text{cm}$ at signal wavelength λ_1 variations. Further increase of λ_1 leads to a drop of $\delta\lambda_3 L$. In

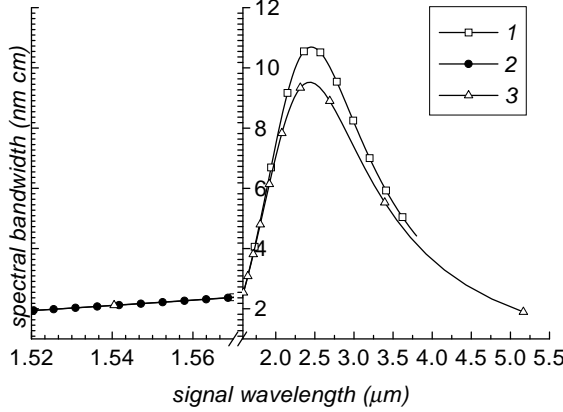


FIG. 3. Phase-matching spectral width as a function of signal wavelength for OPG in KTP crystal at $\lambda_p = 1.064 \mu\text{m}$: 1- $o_3 \rightarrow o_1e_2$ interaction in the x-z plane, 2- $e_3 \rightarrow e_1o_2$, x-y plane, 3- $o_3 \rightarrow e_1o_2$, y-z plane.

the case of xy-plane $e_3 \rightarrow e_1o_2$ interaction $\delta\lambda_p L$ exhibits linear increase up to 2.4 nm·cm under λ_1 variations (curve 2).

It is quite easy to determine from the dependencies given in Figure 3 the acceptance nonmonochromaticity of Nd:YAG laser radiation for type II NPM along x- and y-axis. For KTP crystal of 1 cm length, when signal wavelength λ_1 is equal to $1.57 \mu\text{m}$, the maximal acceptance nonmonochromaticity $\Delta\lambda_3$ is 2.4 nm.

5 Effective nonlinear coefficients in the principal planes of KTP crystal

The effective nonlinear coefficients $d_{eff} = \mathbf{U}^s d : \mathbf{U}^p \mathbf{U}^i$ represent the convolution of the quadratic susceptibility tensor with the unit polarization vector of pump \mathbf{U}^p , signal \mathbf{U}^s and idler \mathbf{U}^i waves [20, 22]. There exist the following nonzero elements of tensor d for the mm2 point group biaxial KTP crystal [24]: d_{15} , d_{24} , d_{31} , d_{32} and d_{33} . The experimental values of $d_{\mu\nu}$ elements are taken from the papers [11, 16]. They satisfy Kleinmann conditions and are equal to $d_{31} = d_{15} = 1.9 \text{ pm V}^{-1}$, $d_{32} = d_{24} = 3.4 \text{ pm V}^{-1}$.

It is simple to show, that the effective nonlinear coefficient for $o_3 \rightarrow o_1e_2$ interaction in the xz-plane is given by the expression

$$d_{eff} = d_{32}U_3^i, \quad (27)$$

where z-axis component of the idler wave unit polarization vector is described by the formula

$$U_3^i = \frac{1}{M_{e2}} \left(N_{x2}^2 - n_{e2}^2(\theta) \cos^2 \theta \right),$$

$$M_{e2} = \left(\left[N_{x2}^2 - n_{e2}^2(\theta) \cos^2 \theta \right]^2 + \frac{1}{4} \left[n_{e2}^4(\theta) \sin^2 2\theta \right] \right)^{\frac{1}{2}}. \quad (28)$$

In the absence of double refraction $N_{x2} = N_{z2}$ and it follows from (24) that $U_3^i = \sin \theta$.

For the $o_3 \rightarrow e_1o_2$ interaction in the yz-plane $d_{eff} = d_{31}U_3^s$, where U_3^s can be found from (28) substituting x by y and index 2 by 1.

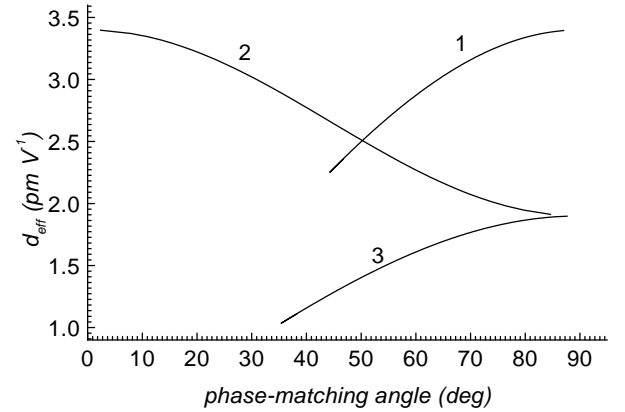


FIG. 4. Effective nonlinear coefficients v.s. phase-matching angle in the principal planes of KTP crystal at $\lambda_p = 1.064 \mu\text{m}$: 1- $o_3 \rightarrow o_1e_2$ interaction in the x-z plane, 2- $e_3 \rightarrow e_1o_2$, x-y plane, 3- $o_3 \rightarrow e_1o_2$, y-z plane.

The effective coefficient for the xy-plane $e_3 \rightarrow e_1o_2$ interaction is given by

$$d_{eff} = d_{31}U_1^p U_1^s + d_{32}U_2^p U_2^s, \quad (29)$$

where

$$U_1^p = (N_{y3}^2 - n_{e3}^2 \cos \varphi) / M_{e3},$$

$$U_2^p = -n_{e3}^2 \sin 2\varphi / M_{e3},$$

$$M_{e3} = \left(\left[N_{y3}^2 - n_{e3}^2(\varphi) \cos^2 \varphi \right]^2 + \frac{1}{4} \left[n_{e3}^4(\varphi) \sin^2 2\varphi \right] \right)^{\frac{1}{2}}. \quad (30)$$

Replacing index 3 by 1 we get from U_1^p, U_2^p the signal wave polarization vector components U_1^s, U_2^s . In the absence of double refraction the equation (29) takes the form: $d_{eff} = d_{31} \sin^2 \varphi + d_{32} \cos^2 \varphi$.

The dependencies of d_{eff} on phase-matching angle in three principal planes of KTP crystal at Nd:YAG laser pumping $\lambda_p = 1.064 \mu\text{m}$ are plotted in Figure 4 (curves 1, 2, 3). It can be seen from Figure 4 that extremal d_{eff} values for the II type OPG are realized in three principal planes of KTP crystal. Besides, OPG of type II in the xz -plane is more efficient than that in the yz -plane. The conversion efficiency along x -axis is $(d_{32}/d_{31})^2$ times higher in comparison with the conversion in y -axis direction.

6 Conclusion

We have analyzed the main types of phase-matching for OPG in the principal planes of KTP crystal with account for dispersion of refractive indices. The polarization types of interacting waves, as well as signal wavelength dependencies on wave propagation directions in the crystal have been also investigated. The estimates of angular and spectral phase-matching widths and effective nonlinear coefficients are presented. These data were used at numerical simulation of nonstationary OPG in the KTP crystal placed in a resonator, in order to obtain the maximal conversion efficiency. These results would be published elsewhere.

Acknowledgments

This work was supported in part by INTAS BELARUS 97-0533.

References

- [1] L.R. Marshall, A. Kaz. J. Opt. Soc. Am. B. **10**, 1730 (1993).
- [2] D.E. Gakhovich, A.S. Grabchikov, V.A. Orlovich et al. SPIE Proc. **2772**, 54 (1996).
- [3] J.D. Bierlein, H. Vanherzeele. J. Opt. Soc. Am. B. **6**, 622 (1989).
- [4] J-F. T. Wang, R. Daneshvar. IEEE J. Quant. Electr. **32**, 183 (1996).
- [5] S.T. Yang, R.C. Eckardt, R.L. Byer. Opt. Lett. **18**, 971 (1993).
- [6] Ch. Grässer, D. Wang, R. Beigang, R.J. Wallenstein. J. Opt. Soc. Am. B. **10**, 2218 (1993).
- [7] A. Nebel, C. Fallnich, R. Beigang, R. Wallenstei. J. Opt. Soc. Am. B. **10**, 2295 (1993).
- [8] L.R. Marshall, A. Kaz, O. Aytur. IEEE J. Quant. Electr. **32**, 177 (1996).
- [9] R. Burnham, R.A. Stolzenberger, A. Pinto. IEEE Photonics Tech. Lett. **1**, 27 (1989).
- [10] L.R. Marshall, A.D. Hays, J. Kasinski, R.L. Burnham. Adv. Sol. State Laser (OSA). **6**, 271 (1990).
- [11] K. Kato. IEEE J. Quant. Electr. **27**, 1137 (1991).
- [12] K. Kato. Opt. Lett. **17**, 178 (1992).
- [13] K. Kato. IEEE J. Quant. Electr. **28**, 1974 (1992).
- [14] L.M. Barkovskii, G.N. Borzdov, F.I. Fedorov. J. Mod. Opt. **37**, 85(1990).
- [15] M.M. Hobden. J. Appl. Phys. **38**, 4365 (1967).
- [16] J.Q. Yao, T.S. Fahlen. J. Appl. Phys. **55**, 65 (1984).
- [17] D.Yu. Serdyukov, V.D. Shigorin, G.P. Shikulo. IEEE J. Quant. Electr. **11**, 1957 (1984).
- [18] B.V. Bokut. Zhurn. Priklad. Spekt. **7**, 621 (1967).
- [19] D.N. Nikogosyan, G.G. Gurzadyan. Kvant. Elektr. **13**, 2519 (1986).
- [20] Y.R. Shen. The Principles of Nonlinear Optics. New York: "Interscience" Publishing. 1984.
- [21] D.A. Roberts. IEEE J. Quant. Electr. **28**, 2057 (1992).
- [22] F. Zernike, J.E. Midwinter. Applied Nonlinear Optics. New York: "Interscience" Publishing. 1973.
- [23] V.G. Dmitriev, G.G. Gurzadyan, D.N. Nikogosyan. Handbook of Nonlinear Optical Crystals. Spr.Ser.in Opt.Sci. 64. Berlin: "Springer-Verlag" Publishing. 1991.
- [24] B. Boulanger, J.P. Feve, G. Marnier et al. J. Opt. Soc. Am. B. **11**, 755 (1994).